HK.NCCP International Journal of Intelligent Information and Management Science
ISSN: 2307-0692, Volume 5, Issue 4, August 2016

Investigation of Multi-cycle Working Process on the Pulse Detonation Engine

Tao JIANG, Chunsheng WENG
National Key Lab of Transient Physics, Nanjing University of Science and Technology, Nanjing 210094, CHINA

Abstract: To investigate multi-cycle working process on pulse detonation engine(PDE), the Euler-Lagrange model considering chemical reaction mechanism for gas-droplets two phase detonation is built, while the gas and liquid equations are respectively calculated by the conservation element and solution element(CE/SE) method and fourth-order Runge-Kutta method. Numerical results show that the multi-cycle working process of PDE is more complicated; with the increase of cycle times, detonation wave propagation velocity increased, the DDT distance and time decreased., until PDE was stable; Due to lack of gasoline caused by the evaporation of gasoline, PDE performance is better when the reactant equivalent is greater than 1.The results have a value to design of pulse detonation engine.

Keywords: Pulse detonation engine; Euler-Lagrange Model; CE/SE method; Two-phase detonation; Atomization; Evaporation; Multi-cycle

1. Introduction

Pulse Detonation Engines(PDE) have been predicted to be more efficient than current aeronautical propulsion systems. They potentially represent a revolutionary propulsion technology that offers advantages in hardware simplicity, operations, and reliability, PDE shows performance advantages in both the subsonic and supersonic flight regimes, PDE is unsteady propulsion devices. They use detonation waves, which allow the chemical energy of the fuel used to be released in a far more rapid manner. The combustion chamber is filled with a fuel/air mixture and detonated. A detonation wave propagates through the chamber creating high pressures that produce thrust. Products of combustion are exhausted and the cycle starts again. Either running this cycle at high frequencies or coordinating multiple combustion chambers can produce quasi-steady thrust.

Venkat [1] et al. simulate the influence of the initial droplet size , droplet evaporation rate and the initial temperature of the initial droplet detonation parameters. Schauer [2] et al. use flash systems to improve the performance of PDE liquid fuel atomization. Varathalrajan [3] et al. studied the influence to speed up the flow rate of liquid fuel atomization within the PDE . Ma Danhua and Peng Zhen [4,5] simulated premixed homogeneous mixture of gasoline and air ignition initiation process by CE / SE method to analyze the inner tube detonation spoiler and a plasma ignition on the impact of the two-phase detonation parameters .

Domestic and foreign scholars have done a lot of research on multi-cycle working process of PDE, but mainly on the ignition process, less on atomization, evaporation and mixing process. To investigate multi-cycle working process on atomization, evaporation and mixing process in pulse detonation engine, the Euler-Lagrange model considering chemical reaction mechanism for gas-droplets two phase detonation is built, while the gas and liquid equations are respectively calculated by the conservation element and solution element(CE/SE) method and fourth-order Runge-Kutta method.

2. Physical Model and Basic Equation

2.1. Physical model

Because the process of gas-liquid two-phase pulse detonation is very complex, we put forward the following assumptions to simplify: Within Pulse detonation engine the flow is axisymmetric ; considering grouped droplets , gasoline was atomizd into spherical droplets in the pulse detonation engine; droplet remain in their initial droplet group and between groups of liquid dropping there is no mass, momentum and energy transfer; in the intake process, part of the gasoline droplet evaporation into gaseous gasoline, then mixed with air; droplet is not broken and keeps a spherical after detonation wave sweep, gasoline vapor occurs chemical reaction with oxygen and release energy.

2.2. Two dimensional axial symmetric gas phase control equations

$$\frac{\partial \boldsymbol{U}}{\partial t}+\frac{\partial \boldsymbol{F}}{\partial x}+\frac{\partial \boldsymbol{G}}{\partial y}=\boldsymbol{R}-\alpha\frac{\boldsymbol{H}}{y} \quad (1)$$

$$\boldsymbol{U}=\begin{bmatrix}\phi_g\rho_g\\ \phi_g\rho_g u_g\\ \phi_g\rho_g v_g\\ \phi_g\rho_g E_g\\ \phi_g\rho_g^1\\ \phi_g\rho_g^2\\ \vdots\\ \phi_g\rho_g^{NI-1}\end{bmatrix}\quad \boldsymbol{F}=\begin{bmatrix}\phi_g\rho_g u_g\\ \phi_g(\rho_g u_g^{2}+p)\\ \phi_g\rho_g u_g v_g\\ \phi_g(\rho_g E_g+p)u_g\\ \phi_g\rho_g^1 u_g\\ \phi_g\rho_g^2 u_g\\ \vdots\\ \phi_g\rho_g^{NI-1}u_g\end{bmatrix}$$

$$\boldsymbol{G}=\begin{bmatrix}\phi_g\rho_g v_g\\ \phi_g\rho_g u_g v_g\\ \phi_g(\rho_g v_g^2+p)\\ \phi_g v_g(\rho_g E_g+p)\\ \phi_g\rho_g^1 v_g\\ \phi_g\rho_g^2 v_g\\ \vdots\\ \phi_g\rho_g^{NI-1}v_g\end{bmatrix}\quad \boldsymbol{H}=\begin{bmatrix}\phi_g\rho_g v_g\\ \phi_g\rho_g u_g v_g\\ \phi_g\rho_g v_g^2\\ \phi_g v_g(\rho_g E_g+p)\\ \phi_g\rho_g^1 v_g\\ \phi_g\rho_g^2 v_g\\ \vdots\\ \phi_g\rho_g^{NI-1}v_g\end{bmatrix}$$

$$\boldsymbol{R}=\begin{bmatrix}\sum I_{d_i}\\ \sum(I_{d_i}u_{l_i}-F_{x_i})\\ \sum(I_{d_i}v_{l_i}-F_{y_i})\\ \sum[-Q_{d_i}+Q_{c_i}-F_{x_i}u_{l_i}+I_{d_i}(E_{l_i}+p/\rho_l)]\\ \rho_c^1+\sum I_{d_i}\delta^1\\ \rho_c^2+\sum I_{d_i}\delta^2\\ \vdots\\ \rho_c^{NI-1}+\sum I_{d_i}\delta^{NI-1}\end{bmatrix}$$

In the form $\alpha=0$ represents two dimensional flow, $\alpha=1$ represents the axial symmetric flow. g and l represent the gas phase and the liquid phase. ϕ_g and ϕ_l is the volume fraction ratio of gas phase and liquid phase, meanwhile $\phi_g+\phi_l=1$. ρ, u, p and T represent density, velocity, pressure and temperature. I_{d_i} is the quality change rate of unit volume.

The force between the gas and the liquid drop in the i group in the unit volume follows[6]:

$$F_{x_i}=n_i f_{dx_i} \tag{2}$$

$$F_{y_i}=n_i f_{dy_i} \tag{3}$$

$$f_{dx_i}=\frac{1}{2}\pi R_i^2 C_D\rho_g\left|\boldsymbol{V}_g-\boldsymbol{V}_{l_i}\right|\left(u_g-u_{l_i}\right) \tag{4}$$

$$f_{dy_i}=\frac{1}{2}\pi R_i^2 C_D\rho_g\left|\boldsymbol{V}_g-\boldsymbol{V}_{l_i}\right|\left(v_g-v_{l_i}\right) \tag{5}$$

$\left|\boldsymbol{V}_g-\boldsymbol{V}_{l_i}\right|=\left[\left(u_g-u_{l_i}\right)^2+\left(v_g-v_{l_i}\right)^2\right]^{1/2}$, Re is Reynolds number, C_D is resistance coefficient:

$$Re=\frac{2\rho_g\left|\boldsymbol{V}_g-\boldsymbol{V}_{l_i}\right|R_i}{\mu_g} \tag{6}$$

$$C_D=\begin{cases}27\,Re^{-0.84} & ,\ Re<80\\ 0.27\,Re^{0.21} & ,\ 80\le Re<10^4\\ 2 & ,\ Re\ge 10^4\end{cases} \tag{7}$$

The equations for chemical reaction[6] is

$$C_8H_{18}+12.5O_2+47N_2=8CO_2+9H_2O+47N_2$$

ρ_g^i is density; δ^i is the percent of contribution of the material source to the component. W_i is molecular weight. In the $\sum_i^{NI}a_i x_i=\sum_i^{NI}b_i x_i$, the relationship of a_i and b_i follows:

$$\sum_i^{NI}(a_i-b_i)\ W_i=0 \tag{8}$$

$$\rho_c^i=W_i\left(b_i-a_i\right)\dot{\omega} \tag{9}$$

$$Q_c=Q_r\dot{\omega} \tag{10}$$

$$Q_r=\sum_i^{NI}\left(a_i-b_i\right)h_i^0 \tag{11}$$

$\dot{\omega}$ is the reaction rate

$$\dot{\omega}=A\left[Fuel\right]^a\left[O_2\right]^b e^{-\left(E_a/R_uT_g\right)} \tag{12}$$

Equation of state

$$p=\sum_{i=1}^{NI}\frac{\rho_g^i}{W_i}T_gR_u \tag{13}$$

Temperature is determined by the following formula:

$$c_vT_g=E_g-\frac{u_g^2+v_g^2}{2} \tag{14}$$

$$c_v=\frac{1}{\rho_g}\sum_{i=1}^{NI}\rho_g^i c_v^i \tag{15}$$

c_v is specific heat at constant volume; c_v^i is the polynomial of temperature;

2.3. Droplet control equation

1) Motion equation of droplet

Dynamic movement is the main reason of drop in pulse detonation engine. Motion equation of droplet is[7]

$$\frac{du_{l_i}}{dt} = \frac{u_g - u_{l_i}}{\tau} \quad (16)$$

$$\frac{dv_{l_i}}{dt} = \frac{v_g - v_{l_i}}{\tau} \quad (17)$$

τ is droplet velocity relaxation time, $\tau = \frac{2\rho_l R_i^2}{9\mu_g f}$ .resistance coefficient $f = \mathrm{Re}\, C_D / 24$.

2) Droplet position equation

$$\frac{dx_i}{dt} = u_{l_i} \quad (18)$$

$$\frac{dy_i}{dt} = v_{l_i} \quad (19)$$

3) Droplet energy equation

According to the law of conservation of energy, the energy absorbed by the liquid drops from the gas is equal to the energy required for the droplet temperature rise and the latent heat required for the liquid to be evaporated. The energy equation of the group i can be written as [7]:

$$\frac{dT_{l_i}}{dt} = \frac{2\pi R_i \lambda_g Nu(T_g - T_{l_i}) - 4\pi R_i^2 \rho_l L \frac{dR_i}{dt}}{4/3\pi R_i^3 \rho_l C_v} \quad (20)$$

4) Droplet atomization model

According to the working characteristics of the pulse detonation engine, the Fipa model [8] is used. The basic idea of this model is that the splitting time of the liquid drop is the basic control parameter of the splitting process, and the time is a function of the droplet Weber number.

Change rate of droplet radius in Fipa model:

$$\frac{dR_i}{dt} = [6\sigma / (\rho_g \left|\boldsymbol{V}_g - \boldsymbol{V}_{l_i}\right|^2) - R_i] / \tau \quad (21)$$

$$\tau = C_1 T_b \varepsilon^{-0.5} (2R_i / \left|\boldsymbol{V}_g - \boldsymbol{V}_{l_i}\right|),\ \varepsilon = \rho_g / \rho_l,\ C_1 = 1.$$

$$T_b = \begin{cases} 6(We_{l_i} - 12)^{-0.25} & ,12 < We_{l_i} \le 18 \\ 2.45(We_{l_i} - 12)^{0.25} & ,18 < We_{l_i} \le 45 \\ 14.1(We_{l_i} - 12)^{-0.25} & ,45 < We_{l_i} \le 351 \\ 0.766(We_{l_i} - 12)^{0.25} & ,351 < We_{l_i} \le 2670 \\ 5.5 & ,We_{l_i} > 2670 \end{cases}$$

5) Droplet evaporation model

According to the working characteristics of the pulse detonation engine, the mixed evaporation model is used. Spalding evaporation model can be used as the intake process is basically a constant process; However, the ignition process is obviously a unsteady process. In this process, the detonation wave speed is very quick, detonation wave sweep outdated droplet evaporation is far greater than the speed of Spalding evaporation model of evaporation rate, stripping evaporation model is applied.

$$\frac{dR_i}{dt} = \begin{cases} -\frac{k}{2\rho_l R_i} \frac{Y_1^* - Y_1}{1 - Y_1^*} Sh_d,\ p > 0.2\mathrm{MPa} \\ -\frac{1}{2}\sqrt{3\pi}\left(\frac{\rho_g \mu_g}{\rho_l \mu_l}\right)^{\frac{1}{6}} \left(\frac{\mu_l}{\rho_l}\right)^{0.5} \left|\boldsymbol{V}_g - \boldsymbol{V}_{l_i}\right|^{0.5} R_i^{-0.5} \\ -\frac{3\lambda Nu\left(T_g - T_{l_i}\right)}{\pi R_i \rho_l L},\ p > 0.2\mathrm{MPa} \end{cases} \quad (22)$$

R_i is a group of the droplet radius i, μ_g and μ_l are the viscosity coefficient of gas phase and liquid phase, respectively. λ_g is the thermal conductivity of gas. L is the heat of vaporization of liquid fuel, C_v is the volume of the liquid phase, Nu is Nusselt number, k is the diffusion coefficient of gas in the air, Y_1^* and Y_1 are gasoline droplet surface and local unit of fuel vapor mass fraction, respectively. Sh_d is the Sherwood number.

6) Droplet impingement model

This paper used the Tabakoff[9]wall model according to the working characteristics of the pulse detonation engine.

$$\frac{v_{n2}}{v_{n1}} = 1.0 - 0.4159\beta_1 - 0.4994\beta_1^2 + 0.292\beta_1^3 \quad (23)$$

$$\frac{v_{t2}}{v_{t1}} = 1.0 - 2.12\beta_1 + 3.0775\beta_1^2 - 1.1\beta_1^3 \quad (24)$$

v_{n1} and v_{t1} respectively are normal and tangential velocity before droplet impingement, respectively. v_{n2} 、 v_{t2} are normal and tangential velocity after droplet impingement, respectively. β_1 is intersection angle between the speed before droplet impingement and wall tangential. β_2 is intersection angle between the speed after droplet impingement and wall tangential. Which is shown in Figure 1.

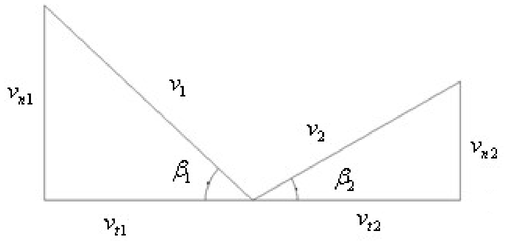

Figure 1. Schematic diagram of droplet and wall collision

3. Calculation Method

3.1. The solution method of gas phase equation

The gas phase equation is calculated by the CE/SE method (the space time conservation element and solution element method), which is first put forward by NASA scientists Chang[10]. It's a new numerical calculation method to solve conservation equations of conservation laws with high precision, strong ability to capture the discontinuous and without the need for Riemann decomposition. Two dimensional CE/SE method is derived from the literature [10], and its calculation format is as follows:

$$\begin{aligned}
&\boldsymbol{U}_{i,j}^{n}-\frac{\Delta t}{2}R_{i,j}^{n}= \\
&\frac{1}{4}\left[\left(\boldsymbol{U}+\frac{\Delta x}{4}\boldsymbol{U}_{x}\right)-\frac{\Delta t}{4}\left(\boldsymbol{G}_{y}-\frac{8}{\Delta x}\boldsymbol{F}-\boldsymbol{F}_{x}-\frac{2\Delta t}{\Delta x}\boldsymbol{F}_{t}\right)\right]_{i-1/2,j}^{n-1/2}+ \\
&\frac{1}{4}\left[\left(\boldsymbol{U}-\frac{\Delta x}{4}\boldsymbol{U}_{x}\right)-\frac{\Delta t}{4}\left(\boldsymbol{G}_{y}+\frac{8}{\Delta x}\boldsymbol{F}-\boldsymbol{F}_{x}+\frac{2\Delta t}{\Delta x}\boldsymbol{F}_{t}\right)\right]_{i+1/2,j}^{n-1/2}+ \\
&\frac{1}{4}\left[\left(\boldsymbol{U}+\frac{\Delta y}{4}\boldsymbol{U}_{y}\right)-\frac{\Delta t}{4}\left(\boldsymbol{F}_{x}-\boldsymbol{G}_{y}-\frac{8}{\Delta y}\boldsymbol{G}-\frac{2\Delta t}{\Delta y}\boldsymbol{G}_{t}\right)\right]_{i,j-1/2}^{n-1/2}+ \\
&\frac{1}{4}\left[\left(\boldsymbol{U}-\frac{\Delta y}{4}\boldsymbol{U}_{y}\right)-\frac{\Delta t}{4}\left(\boldsymbol{F}_{x}-\boldsymbol{G}_{y}+\frac{8}{\Delta y}\boldsymbol{G}+\frac{2\Delta t}{\Delta y}\boldsymbol{G}_{t}\right)\right]_{i,j+1/2}^{n-1/2}
\end{aligned} \tag{25}$$

3.2. The solution method of liquid drop equation

Droplet equation (16) to (22) are ordinary differential equations. A lot of methods are used to solve ordinary differential equations, such as Newton iterative method, integral equation method and four order Runge Kutta method. Considering the stability and computing the tradeoff between accuracy and computational efficiency, this paper adopts variable step size fourth-order Runge Kutta method to solve the droplet equation.

3.3. Source terms

The characteristic time of chemical reaction caused by droplet evaporation is much less than that of the characteristic time of convection, so the source term is rigid in the computation of two-dimensional CE/SE method. In this paper, using the four order Runge Kutta method to deal with stiff source term. First without considering the effect of the source term R, the CE/SE method is used to solve $(\boldsymbol{U})_j^n$, and then used $(\boldsymbol{U})_j^n$ as the initial value, solution of ordinary differential equations $d\boldsymbol{U}/dt=\boldsymbol{R}$. Time step four order Runge Kutta method in desirable:

$$\Delta t_{R-K}=\frac{\Delta t_{CE/SE}}{2N}$$

3.4. Initial conditions

The pipe length of PDE is 120mm,the inner diameter is 80mm,We just need to take only half the calculation area and divide the mesh into 1200x40 cells because of the tube flow field of PDE is axisymmetric. Air inlet for the axial inlet, let the tube initial axial flow rate of the first cycle of PDE be 100m/s, and the radial velocity be 0m/s;Gasoline is divided into N droplet groups, the size of the droplet after leaving the nozzle is distributed by Rosin - Rammler .Sauter mean diameter is100,initial temperature of the droplet is 298K.Set a temperature of 600 k high temperature when the ignition begins,High temperature is 180 mm - 220 mm from the thrust wall and 0-20mm from the wall.

3.5. The boundary conditions

The PDE solid wall boundary uses specular reflection boundary conditions, export free boundary using CE/SE method of reflection boundary conditions, on the central axis using axisymmetric boundary conditions for processing. When the inlet valve is opened, we use inlet boundary conditions here; When the inlet valve is closed, we use mirror reflection boundary conditions here. Multi-cycle isolation in pulse detonation engine simulation process using the left end face filling isolated gas inflow model, The isolation and filling conditions is to keep the total pressure of gas be 0.1893Mpa,keep the total temperature be 308K at the same time. Axial velocity by interior point interpolation, When the detonation tube of gas volume fraction on exit to stoichiometric ratio under the condition of the corresponding values, enter the detonation process.

4. Discussion

4.1. The solution method of gas phase equation

An entire working cycle of pulse detonation engine includes 6 basic procedures:

①The filling process of fuel/oxidizer

Figure 2 shows the distribution of average SMD diameter of gasoline droplets after filling PDE tube. Figure 3

International Journal of Intelligent Information and Management Science
ISSN: 2307-0692, Volume 5, Issue 4, August 2016

shows the curve of gasoline SMD radius with axis at different inlet air temperatures. Figure 4 shows the curve of gasoline mass in cross section with axis in PDE tube. As figure2-4 described, from the exit of nozzle to 0.1m away from thrust wall, gasoline droplets are atomized rapidly by the impact of axial flow because of the great speed difference of gas and liquid. The average SMD radius of gasoline droplets is reducing as the secondary atomization. Whereas, the percentage of gasoline vapor mass is relatively small and droplet evaporation has little impact on its radius. Thus, the average SMD radius of gasoline droplets is 59.3 μm at the cross section 0.1m away from thrust wall. From the area which is 0.1m away from thrust wall, the crash of droplets to wall causes the loss of kinetic energy. And then, the reducing of the velocity difference between gas and liquid leads to the slowing down of secondary atomization. However, because the droplets are filling in the cross section, the interact of gas and liquid causes the increasing of evaporating velocity of gasoline due to absorbing gas energy. At the same time, the crash of droplet emerges produces a large number of smaller size droplets, which is beneficial to evaporating. The average SMD radius of gasoline droplets is 32.8 μm at the cross section 0.5m away from thrust wall. Through the remixing of gas and liquid in the first half tube, the velocity and temperature differences between gas and liquid are diminishing and the changing trend of gasoline droplets SMD radius is slowing down. The average SMD radius of gasoline droplets is 30.1 μm at the exit of PDE tube.

②Firing process:

③The formation and steady propagation of detonation wave:

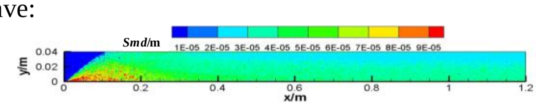

Figure 2. The distribution of average SMD diameter of gasoline droplets after filling PDE tube

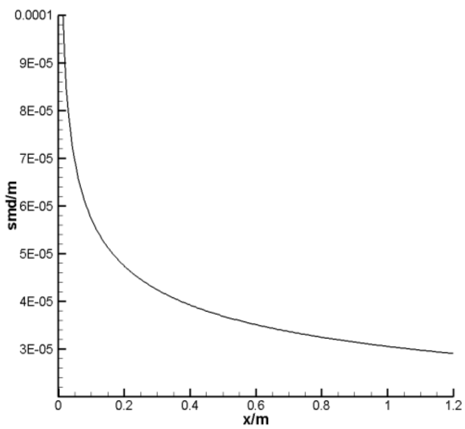

Figure 3. The curve of gasoline SMD radius with axis at different inlet air temperatures

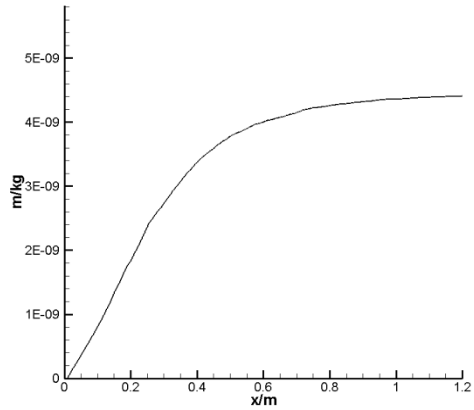

(a) The mass of gasoline vapor

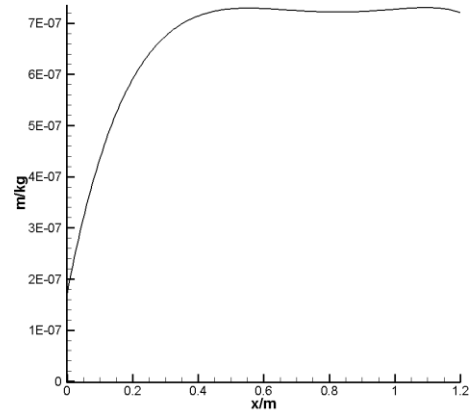

(b) The total mass of gasoline

Figure 4. The curve of gasoline mass in cross section with axis in PDE tube

Figure 5 shows the pressure distribution in detonation tube at different time after firing. After explosive mixture filling the entire tube, firing system ignites the mixture. The ignition zone is a high temperature region. Gasoline vapor in the area is ignited and has a quick interact with oxygen to produce large energy to increase the temperature and pressure of this region to speed up the evaporation rate of liquid drop of gasoline. At the same time, the high temperature and high pressure region is enlarged, and the combustion wave is spread to the surrounding area in circular form. At 36.3 μs , the combustion wave reaches the axial line (Fig 5(a)). The intensity of combustion wave along the axial motion is gradually weaken (Fig5(b)-(d)). Due to the constraints of the pipe wall and the impact of the collision, the radial combustion wave forms a detonation center at the position of 0.32m away from the thrust wall near the axis(Fig5(f), p=3.4MPa) and the reflection wave moving to wall. The center of detonation is moving upward with the reflection wave, which cause the transient evaporation via region. The mixture reaction rate of the chemical reaction is accelerated, and the high pressure area is constantly expanding. Under the constraint of the wall surface of the detonation tube, the upper and lower motion of the detonation center and the reflected wave continue to enhance the strength of the leading shock wave. Eventually at 447.1 μs and at the position of 0.86m away from the thrust wall, it is developed into a transverse detonation wave filling the cross section of detonation tube(Fig5(i), p=2.5MPa). As figure 5 shown, at the exit of PDE tube, the peak pressure of detonation wave is 2.4MPa. By the comparison of Fig 5(i) and Fig 5(j), the difference of detonation wave pressure peak value is small, and the distribution of pressure value is basically the same. That means a self-sustaining propagation detonation wave has formed in the tube.

④The expansion wave propagation process:

⑤The process of exclusion of the combustion products:

⑥The filling process of isolator:

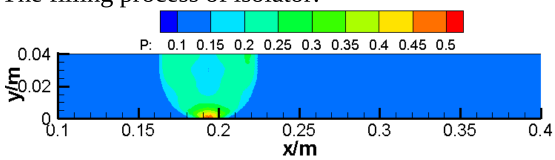

(a)36.3 μs

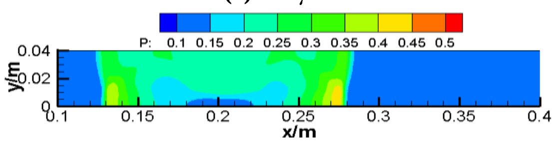

(b)131.4 μs

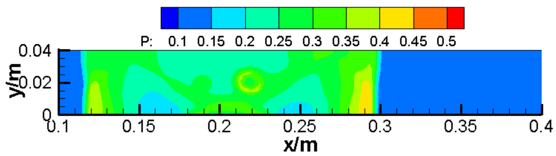

(c)154.9 μs

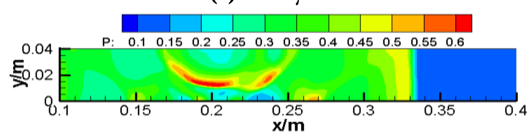

(d)200.8 μs

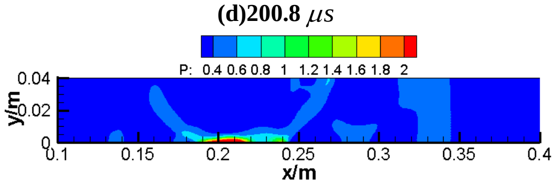

(e) 217.9 μs

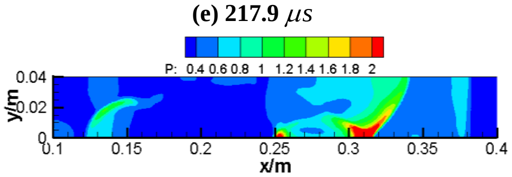

(f)261.5 μs

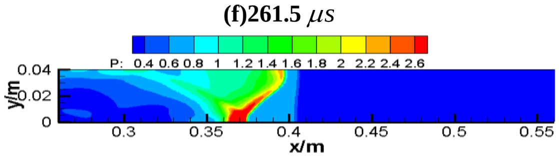

(g) 286.5 μs

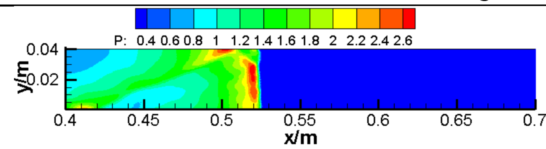

(h) 352.3 μs

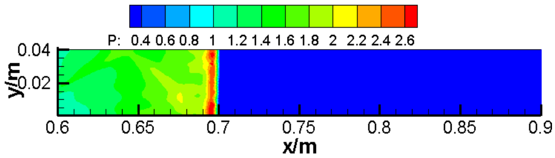

(i) 447.1 μs

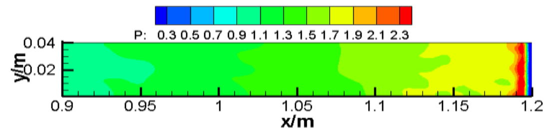

(j) 712.21 μs

Figure 5. The pressure distribution in detonation tube at different time after firing

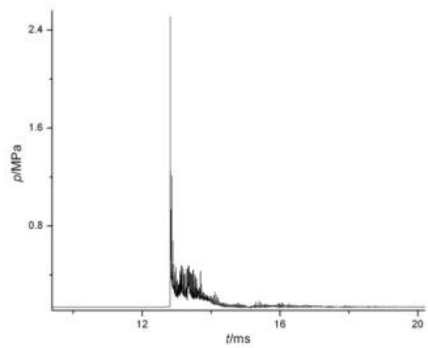

Figure 6. p-t curve at the exit of PDE

The peak pressure decreases rapidly after detonation wave propagates outside the tube, and expansion wave propagates reversely into the detonation tube. When expansion wave reaches the thrust wall, it reflects into another group of reflection wave spreading toward the opening end, and clearing the detonation tube combustion product tube. When the pressure in the tube is reduced to a certain value, isolation gas is used to isolate the high-temperature combustion products which is not clear completely.

4.2. The influence of multi-cycle on the working process of PDE

In this section we will analyze the difference of each multi-cycle PDE's working process.

Table 1 gave out the average temperature of PDE tube before ignition. As can be seen from the table 1, from the first cycle to the seventh cycle, the average temperature of the tube steadily increased, after the seventh cycle the average temperature remained unchanged. Fig. 7 is the curves of the Sauter mean radius of gasoline droplets with the axis of the tube in different cycles. As can be seen from Figure 7, with the increase of cycle times, the Sauter mean radius of gasoline droplets drop faster along the axis, and as a result the Sauter mean radius of the droplets in the PDE tube outlet get smaller. The Sauter mean radius of droplets in the PDE tube exit were 30.1, 28.9, 27.4 and 26.5 in cycle 1, cycle 3, cycle 5 and cycle 7. With the increase of cycle times, average temperature in the tube increases, and it will result in larger temperature difference between gas and liquid phase while the inlet oil temperature keeping invariant. This is conducive to the gasoline droplet evaporation. The Sauter mean radius will decrease more quickly. While tube gasoline vapor quality and mass fraction increase. However, because of the droplet follow feature is not good, in the same filling time, remaining total gasoline quality in the tube is the smallest. After the seventh cycles, the mixing process of atomization and evaporation tends to be stable.

Table 1. The average temperature of PDE tube before ignition

Cycle times	1	3	5	7	8	10
Average temperature (K)	298	318	337	345	346	344

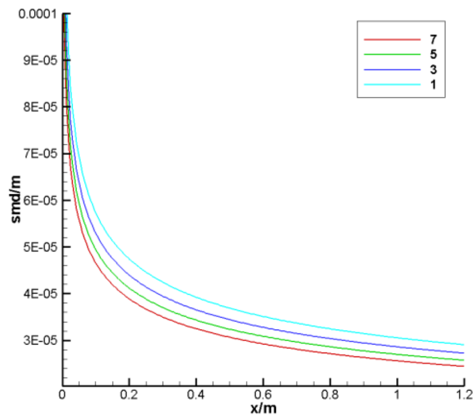

Figure 7. Change curves of the Sauter mean radius of gasoline droplets with the axis of the tube in different cycles

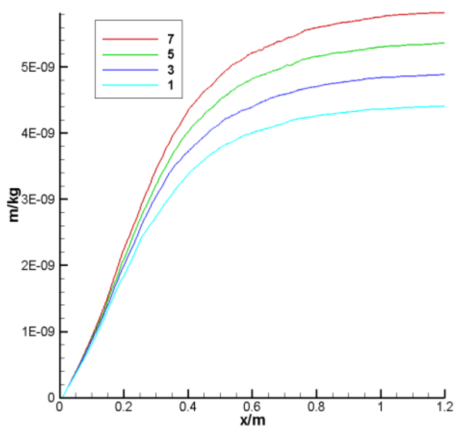

(a) Gasoline vapor quality

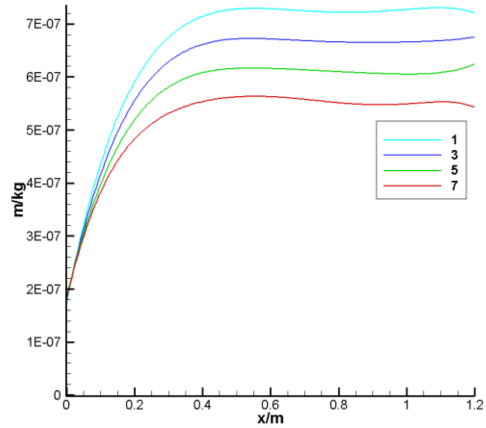

(b) Total gasoline quality

Figure 8. Change curves of gasoline quality with the axis of the cross section of PDE tube in different cycles

Table 2. Detonation parameters in different cycles

Cycle times	Peak pressure of detonation wave (MPa)	Detonation wave propagation velocity (m/s)	DDT distance(m)	DDT time(ms)
1	2.48	1778	0.86	0.674
3	2.33	1852	0.80	0.628
5	2.23	1972	0.75	0.556
7	2.07	2034	0.70	0.539

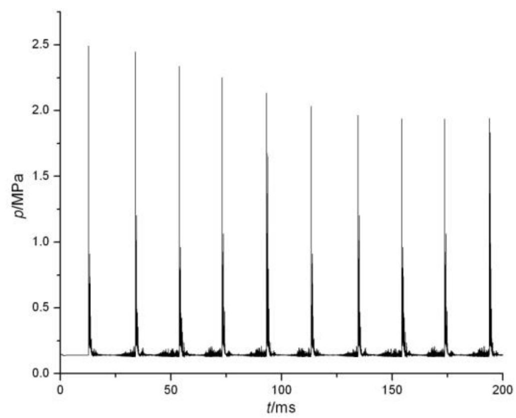

Figure 9. p-t curve at axis of PDE exit

From Table 2 we can see that with the increase of cycle times, droplet radius decreased, gasoline vapor mass fraction increased, the rate of chemical reaction accelerated, detonation wave propagation velocity increased, the DDT distance and time decreased. However when more oxygen remained after detonation waves swept, the condition of lean fuel getting harder in the tube, so the detonation wave peak pressure decreased. After the seventh cycle, peak pressure of detonation wave remained stable and the DDT distance and time kept constant. These features declared that the pulse detonation engine tends to be stable.

The results show: with the increase of cycle times, detonation wave propagation velocity increased, the DDT distance and time decreased., until PDE was stable. Due to lack of gasoline caused by the evaporation of gasoline, PDE performance is better when the reactant equivalent is greater than 1.

5. Acknowledgment

Results of the numerical study on the straight work process of multi cycle show:

1. The multi-cycle work process of PDE was more complicated
2. With the increase of cycle times, detonation wave propagation velocity increased, the DDT distance and time decreased., until PDE was stable.
3. Due to lack of gasoline caused by the evaporation of gasoline, PDE performance is better when the reactant equivalent is greater than 1.

References

[1] Venkat E. Investigations of Two-phase Detonations For Performance Estimations of a Pulse Detonation Engine [R]. AIAA Paper,2007-1173

[2] Lasheras J, Varatharajan B, Varga C, et al. Studies of Fuel Distribution and Detonation Chemistry for Pulse Detonation Engines [R]. ISABE,2001-1174

[3] Christen L. Miser, Paul I. King. PDE Flash Vaporization System for Hydrocarbon Fuel Using Thrust Tube Waste Heat [R]. AIAA Paper,2005-3511

[4] Ma Danhua, Weng Chunsheng. Numerical investigation of two-phase detonation with the obstacles [J]. Journal of Propulsion Technology , 2011,32(3): 425-430

[5] [Peng Zhen, Weng ChunSheng. Numerical calculation of plasma ignition on Pulse Detonation Engine[J]. Engineering Mechanics,2011, 32(3): 425-430

[6] Hong Tao. Theoretical and numerical study of detonation in two-Phase systems [D]. Mianyang, China Academy of Engineering Physics, 2004, 38-39

[7] Liu Ning, Zhang Xiangyan. Theory and numerical simulation of spray combustion process in regenerative liquid propellant guns [J]. Engineering Mechanics,2009, (3): 224-228

[8] Habchi C, Verhoeven D， Huu C H, et al. Modeling atomization and breakup in high-pressure diesel fuel sprays [C]. SAE Paper,1997-0881

[9] Nie Wansheng, Feng Songjiang. Liquid rocket engine combustion kinetics model and numerical calculation [M].Beijing:National Defense Industry Press,2011:70

[10] Weng Chungsheng,Wang Hao. Computational interior ballistics [M]. Beijing: National Defense Industry Press, 2006,188~189